Supplementary Information for "Light trapping beyond the ergodic limit"

Energy density and local absorption rate

The electromagnetic energy density can be expressed in terms of the local density of optical states (LDOS), the modal occupation number, and the energy of each mode,

$$U(\omega) = \rho(r,\omega) \cdot \langle \nu \rangle \cdot \hbar\omega \tag{1}$$

In a homogeneous environment with refractive index, n, and with purely thermal Bose-Einstein occupation, the electromagnetic energy density takes the familiar form:

$$U(\omega) = \frac{n^3\omega^2}{\pi^2 c^3} \cdot \frac{1}{e^{\frac{\hbar\omega}{kT}} - 1} \cdot \hbar\omega \tag{2}$$

Because we are interested in solar cells, it is useful to relate our well-known and easily calculable expression for energy density to absorption. We do this through the commonly used expression for the local absorption rate:

$$A(r,\omega) = \frac{1}{2}\omega \cdot \varepsilon''(r) \cdot E(r)^2 \tag{3}$$

The absorption can be related to the energy density through the electric field intensity. In the limit of a lossless, dispersionless medium:

$$U(r,\omega) = \frac{1}{2}\varepsilon(r,\omega)\cdot E(r,\omega)^2 + \frac{B(r,\omega)^2}{2\mu(r,\omega)} = \varepsilon(r,\omega)\cdot E(r,\omega)^2 \tag{4}$$

Equating these two expressions for the energy density (Eq. [1] and Eq. [4]) and rearranging, we have for the electric field intensity,

$$E(r,\omega)^2 = \frac{1}{\varepsilon(r,\omega)}\rho(r,\omega)\cdot\langle\nu\rangle\cdot\hbar\omega \tag{5}$$

We can insert this into Eq. [3] to determine how the LDOS and modal occupation number affect the local absorption rate,

$$A(r,\omega) = \frac{1}{2\varepsilon(r,\omega)}\varepsilon''(r,\omega)\cdot\rho(r,\omega)\cdot\langle\nu\rangle\cdot\hbar\omega^2 \tag{6}$$

Because Eq. [1] and Eq. [4] assume lossless materials, we can only introduce a small amount of absorption before these concepts become ill-defined. To gain insight, it is nevertheless common to use expressions like these in the limit of low absorption to describe light trapping phenomena, as has been done both in the original derivation[1] and subsequent treatments[2,3] . We will find next, however, that Eq. [6] is not necessary but rather has been used to verify the importance of energy density ratios. As with the expressions for energy density, we can now take the ratio of local absorption rate for two distinct cases of interest,

$$\frac{A(r,\omega)_{case1}}{A(r,\omega)_{case2}} = \frac{\rho(r,\omega)_{case1}\cdot\langle\nu\rangle_{case1}}{\rho(r,\omega)_{case2}\cdot\langle\nu\rangle_{case2}} \tag{7}$$

Which is the same result obtained before from the energy densities, supporting the importance of this ratio.

Recovering the Yablonovitch limit

For a bulk, homogeneous slab of semiconductor with a planar interface, light incident from all 2π steradians gets coupled into a small subset of the modes within the slab given by the escape cone defined by Snell's law. We call these radiation modes. We assume that all incident light is transmitted to the solar cell, thus each of these radiation modes is fully occupied with the maximum occupation number defined through the modified radiance theorem[2,4]. Each incident mode contains an occupation number, $\langle\nu\rangle_{inc}$, and is mapped into a single radiation mode within the semiconductor defined by Snell's law with maximum occupation number[2,4] $\langle\nu\rangle_{max} = \langle\nu\rangle_{inc}$. No more light can be coupled into these radiation modes within the slab as they are fully occupied to the maximum extent dictated by thermodynamics. There are of course $4\pi - \theta_c$ modes inside the semiconductor left unoccupied in this case, where θ_c is the critical angle for total internal reflection, and we call these trapped or evanescent modes[2]. These trapped modes are inaccessible from free space without a momentum changing event such as scattering or diffraction. We count the number of excitations within the slab by multiplying the number of modes accessed by their occupation number.

We now look at the same slab of semiconductor with a Lambertian scattering surface. We assume that this surface does not alter the density of states within the slab as is often assumed[1,2]. This means that in the ratio of Eq. [7], the LDOS terms will cancel, and we will be left with only the ratio of the modal occupation numbers. For an incident mode with occupation number $\langle\nu\rangle_{inc}$, the scattering event splits the energy in this mode equally between all modes within the semiconductor. Thus, each of the internal modes, both radiation and trapped, now have a fraction of this energy, corresponding to $\langle\nu\rangle_{inc}/2\pi$. This means that each of the internal modes can be fed more energy as their occupation numbers are not at their maximum value. We can continue to couple light into the semiconductor until each of these 4π internal modes has an occupation number $\langle\nu\rangle_{max} = \langle\nu\rangle_{inc}$. We again count the

number of excitations by multiplying the number of modes by their occupation numbers. Now using this Lambertian structure, Eq. [7] becomes,

$$\frac{\rho_{lambertian}\langle \nu \rangle_{lambertian}}{\rho_{planar}\langle \nu \rangle_{planar}} = \frac{\langle \nu \rangle_{lambertian}}{\langle \nu \rangle_{planar}} = \frac{4\pi \langle \nu \rangle_{inc}}{\theta_c \langle \nu \rangle_{inc}} = \frac{4\pi}{\theta_c} \approx 4n^2 \quad (8)$$

where we have assumed integration over all modes of the structure. This results in the traditional ergodic light trapping limit.

GaP/CdSe/GaP slot solar cell

We perform a similar calculation to Fig. 2d using realistic, all inorganic materials. For the cladding layer we use the weakly absorbing indirect semiconductor GaP and for the core we use CdSe. These materials fit the criterion that the refractive index of the core is lower than that of the cladding for all wavelengths of interest. In Fig. S1 we plot the spatially averaged LDOS enhancement within the CdSe slot for various slot thicknesses. It can be seen that over all wavelengths of interest there is an increased LDOS due to the slot waveguide effect, becoming more pronounced as the slot thickness is reduced.

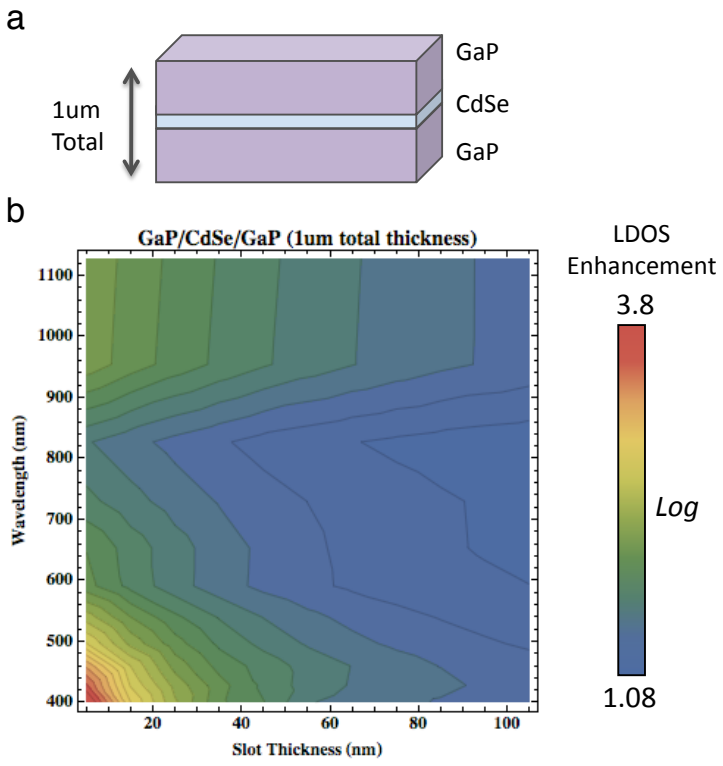

Figure S1: **(a)** Schematic of slot waveguide structure using realistic materials GaP and CdSe. **(b)** Averaged LDOS enhancement within the CdSe slot as a function of slot thickness with a constant total device thickness of 1um.

Photonic crystal enhanced solar cell

There are a least two ways that photonic crystals can be taken advantage of for solar cells. A photonic crystal could be carved out of a bulk, planar solar cell, or an unstructured, planar solar cell could be integrated with a photonic crystal. The former is certainly intriguing as large LDOS enhancements would be expected but has issues regarding increased surface recombination associated with nanostructuring the active region. Still, utilizing a liquid junction[5] or appropriate passivation of a solid state surface[6] could solve this problem. Here we consider integrating a non-absorbing planar photonic crystal with an unstructured, planar solar cell. This could be easily realized by making the photonic crystal out of an anti-reflection coating material such as SiN_x, ZnS, or TiO_2, or by patterning a window

layer such as AlGaAs or InGaP on a III-V solar cell such as GaAs. Here, we take a material of index 3.7, common for III-V materials like GaAs, InGaP, and AlGaAs, and create a hexagonal lattice of air holes in it with a radius of 205 nm and lattice contant of 470 nm. These parameters are designed so that there is a slow mode with high density of states at the GaAs bandedge of 870 nm. We put this photonic crystal on a thin 10 nm planar layer of the same material and calculate the LDOS with FDTD[7] as a function of position in the middle of the 10 nm plane. In Fig S2 it can be seen that there are significant LDOS enhancements at various positions throughout the structure. In Fig S3 we also show the spatial LDOS profiles for select wavelengths. It can be seen that at the bandedge and within the visible part of the spectrum there are significant LDOS enhancements and a supression of the LDOS within the photonic bandgap starting at 870 nm.

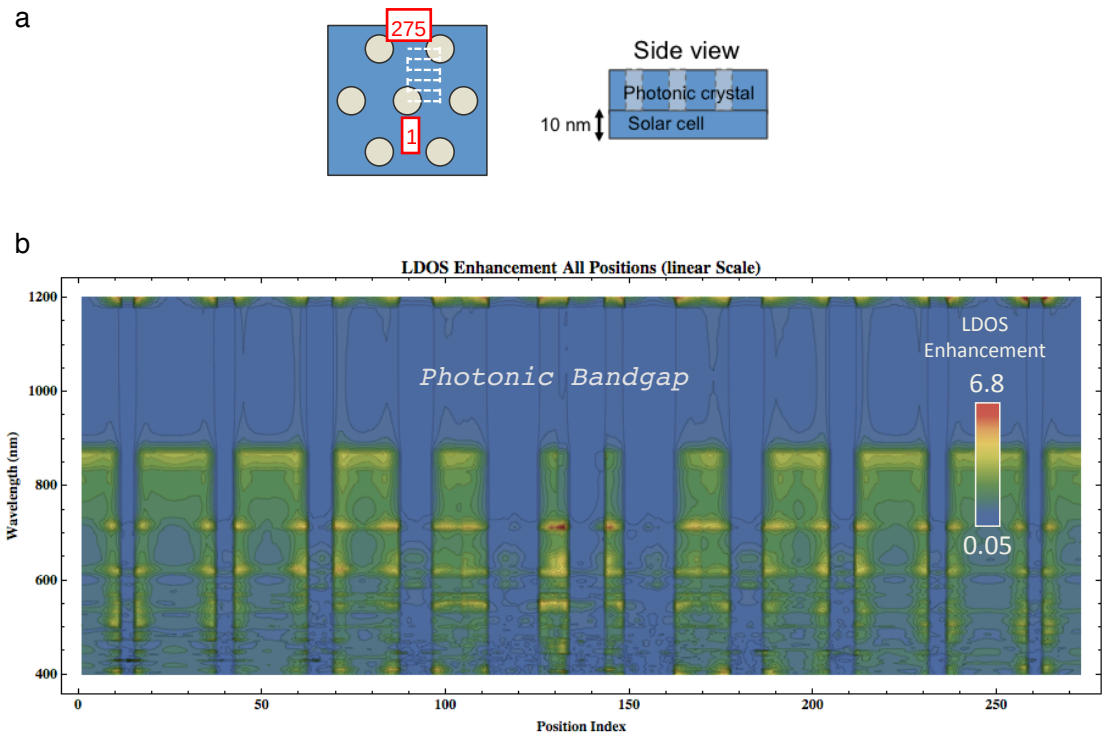

Figure S2: **(a)** Top and side view schematic of the photonic crystal solar cell simulated. **(b)** LDOS map as a function of wavelength and position along the white dotted like shown within the schematic in **(a)**.

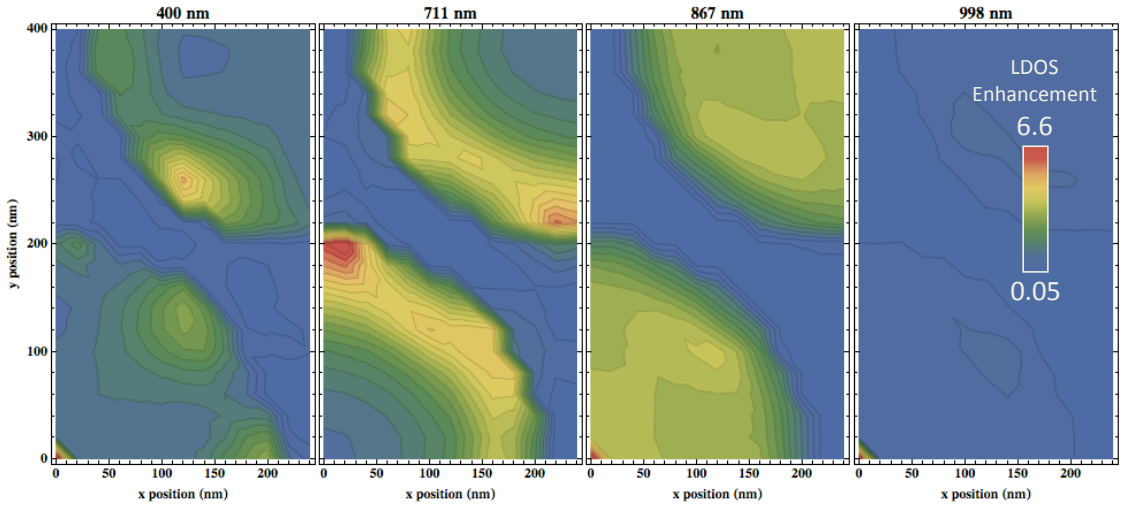

Figure S3: Spatial maps of the LDOS enhancement within the center of the 10nm planar layer of dielectric at various wavelengths.

Sum rule and spectral reweighting

For a solar cell of material index n, absorption coefficient α, and thickness x, the density of states needed to absorb all of the incident radiation is given by:

$$\rho_{\max} = \frac{\rho_{bulk}}{\left(1 - e^{-\alpha(4n^2)x}\right)}, \tag{9}$$

where $\rho_{bulk} = n^3\omega^2 / \pi^2 c^3$ is the homogeneous density of states of the bulk material. Recall the sum rule:

$$\int_0^\infty \frac{\rho_{cell} - \rho_{vac}}{\omega^2} d\omega = 0 \tag{10}$$

.

If the cell is to absorb all of the incident light over the spectral range from ω_0 to ω_1, e.g. over the solar spectrum, then over this range, $\rho_{cell} \rightarrow \rho_{\max}$. By the sum rule, over some other spectral range, ω_2 to ω_3, the density of states of the cell must be reduced. If n and α are approximately constant over the range ω_0 to ω_1 and n is constant over

ω_2 to ω_3, then the minimum bandwidth of the suppression region, ω_3-ω_2, corresponds to:

$$\left(\omega_3 - \omega_2\right) = \frac{\left(\omega_1 - \omega_0\right)}{\left(e^{-\alpha(4n^2)x} - 1\right)}. \qquad (11)$$

Fully populating the modes of the structure

We now briefly discuss the importance of fully populating the modes of the arbitrarily designed solar cell structure. As the ratio of equation (2) indicates, a structure with an elevated LDOS is necessary but not sufficient to exceed the light trapping, which also depends on the modal occupation numbers. There are numerous examples of solar cell structures that very likely have an elevated LDOS; however, whether or not they have exceeded the traditional light trapping limit has remained uncertain[8,9]. Structures that use diffractive elements such as gratings and photonic crystals often couple into only a small subset of the available modes, dictated by momentum conservation. This severely limits the number of modes that are occupied, much like the above-mentioned case of a planar interface. If these structures were integrated with a scattering layer, the full modal spectrum of the device could in principle be excited, and much more light could be absorbed within the solar cell. This would also resolve the relevant problem of limited angular and polarization response associated with many designs. We also note that full modal occupation is not necessary to surpass the ergodic limit as shown using FDTD calculations.

Exceeding the $4n^2$ limit with a slot waveguide

Adding a back reflector to the structure in Fig. 4a increases the ergodic limit for light absorption enhancement to from $2n^2$ to $4n^2$. We show in Fig. S4 that this $4n^2$ limit can also be exceeded with the GaP clad layer of 10nm P3HT:PCBM over substantial wavelength ranges.

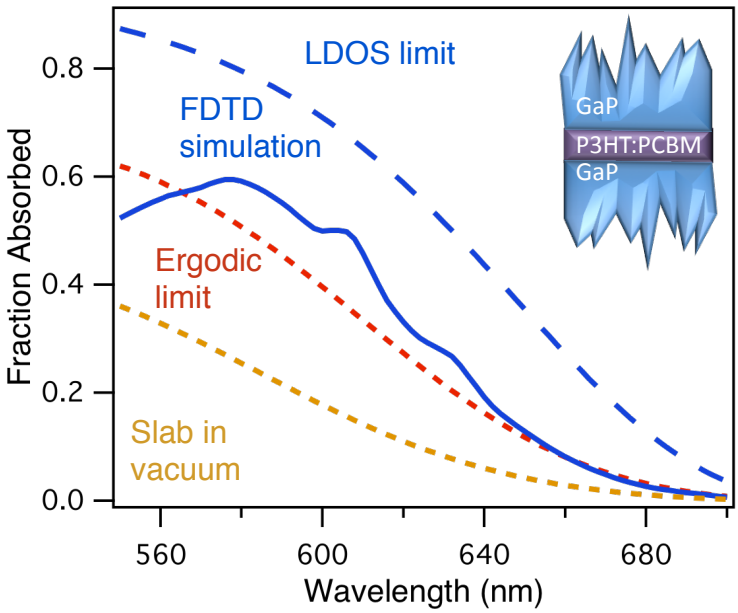

Figure S4: 3D FDTD calculated absorption spectra of a 10nm layer of P3HT:PCBM clad with 500nm of GaP on each side above a metal back reflector. The ergodic limit in this case is 2 times higher than that without a back reflector, but is still exceeded with this structure over a substantial wavelength range.

Angular response of a roughened slot waveguide structure

The original ergodic limit calculation assumed isotropic illumination. We thus calculate the angular response of our slot waveguide test structure to ensure that the ergodic limit is surpassed when averaged over all angles. Figure S5 shows the

fraction absorbed for two wavelengths as a function of angle of incidence, averaged over both polarizations. The ergodic limits for each wavelength are also shown as dashed lines. The limit is exceeded for most angles for each of the wavelengths, falling off only at very steep incidence as expected. The angle averaged absorbances for 550 nm and 600 nm light are 0.48 and 0.34, respectively, indicating that the ergodic limit is surpassed with this structure even with isotropic illumination.

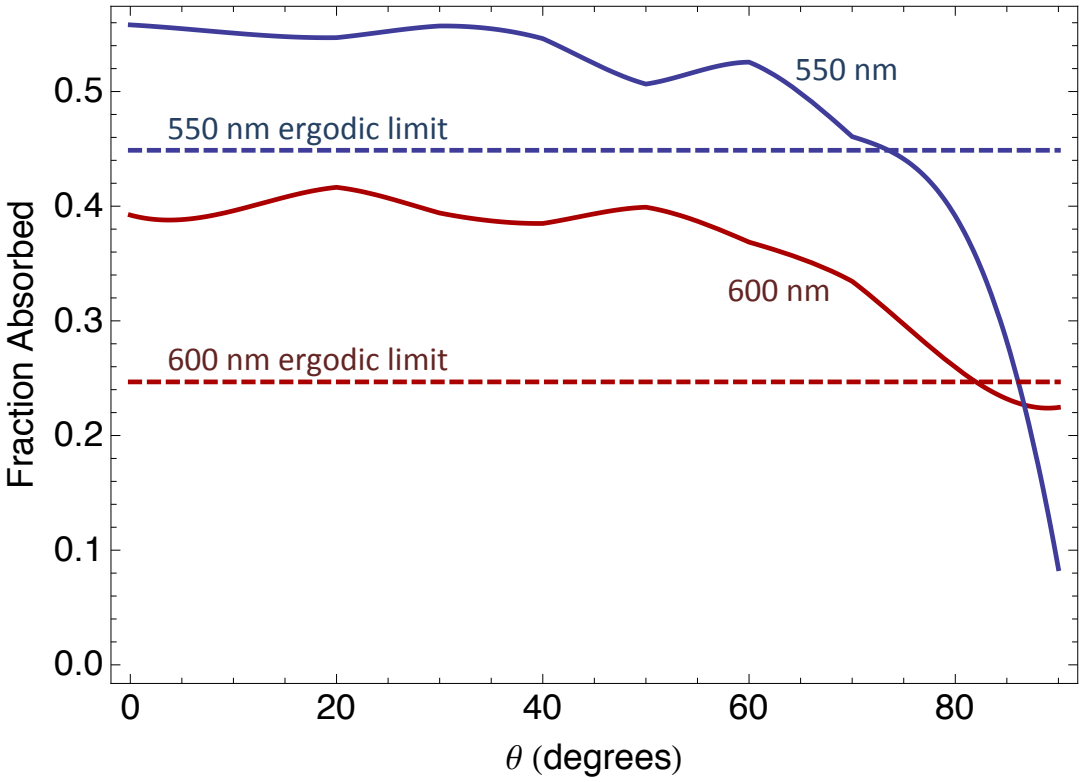

Figure S5: Fraction of incident light absorbed as a function of incidence angle for 550 nm (blue) and 600 nm (red) light. The respective ergodic limits are also shown as dashed lines for each wavelength.

Exceeding the ergodic limit with plasmonics

Adding plasmonic elements to a solar cell can greatly increase the LDOS within the active layer if designed properly. A planar metallic back reflector supports surface plasmon polaritons (SPPs), but these are difficult for designing broadband, angle insensitive incouplers. Alternatively, the cavity effect can be combined with plasmonics to design localized plasmonic resonators with exceedingly high LDOS. With all plasmonic designs, there is the added challenge of overcoming ohmic loss in the metal. In some cases, this can be overcome as shown in Fig. S6. For three different configurations of periodic Ag resonators cladding a 10 nm P3HT:PCBM layer, the ergodic limit is exceeded at normal incidence over a tunable range of wavelengths.

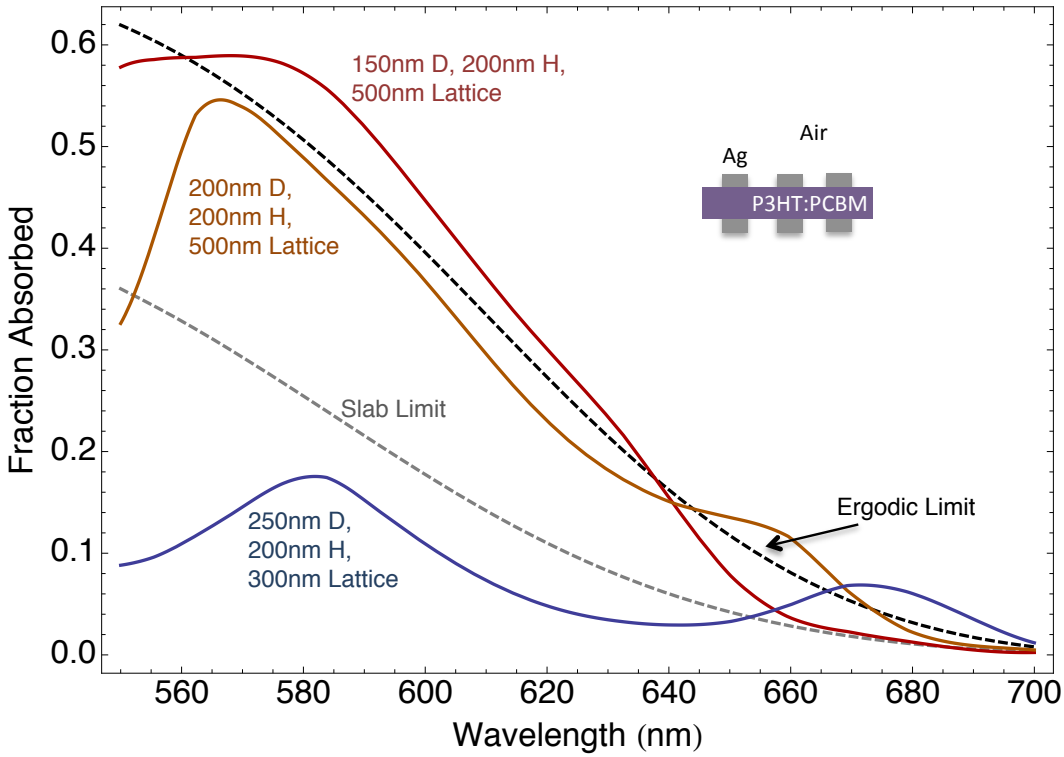

Figure S6: 3D FDTD calculated absorption spectra of a 10nm layer of P3HT:PCBM clad with various arrays of plasmonic Ag resonators. Depending on the resonator diameter (D), height (H) and lattice spacing, the ergodic limit can be exceeded over different portions of the spectrum.

1 Yablonovitch, E. Statistical ray optics. *J. Opt. Soc. Am.* **72**, 899-907 (1982).
2 Stuart, H. R. & Hall, D. G. Thermodynamic limit to light trapping in thin planar structures. *J Opt Soc Am A* **14**, 3001-3008 (1997).
3 Yu, Z. F., Raman, A. & Fan, S. H. Fundamental limit of nanophotonic light trapping in solar cells. *P Natl Acad Sci USA* **107**, 17491-17496, doi:Doi 10.1073/Pnas.1008296107 (2010).
4 Bassett, I. M. Limits to Concentration by Passive Means. *Opt Acta* **32**, 1577-1592 (1985).
5 Boettcher, S. W. *et al.* Energy-Conversion Properties of Vapor-Liquid-Solid-Grown Silicon Wire-Array Photocathodes. *Science* **327**, 185-187, doi:Doi 10.1126/Science.1180783 (2010).
6 Yablonovitch, E., Allara, D. L., Chang, C. C., Gmitter, T. & Bright, T. B. Unusually Low Surface-Recombination Velocity on Silicon and Germanium Surfaces. *Phys Rev Lett* **57**, 249-252 (1986).
7 Koenderink, A. F., Kafesaki, M., Soukoulis, C. M. & Sandoghdar, V. Spontaneous emission in the near field of two-dimensional photonic crystals. *Opt Lett* **30**, 3210-3212 (2005).
8 Chutinan, A., Kherani, N. P. & Zukotynski, S. High-efficiency photonic crystal solar cell architecture. *Opt Express* **17**, 8871-8878 (2009).
9 Garnett, E. & Yang, P. Light Trapping in Silicon Nanowire Solar Cells. *Nano Letters* **10**, 1082-1087, doi:10.1021/nl100161z (2010).